Research Paper

PAIN 164 (2023) 2463–2476

PAIN®

OPEN

Morphine-induced osteolysis and hypersensitivity is mediated through toll-like receptor-4 in a murine model of metastatic breast cancer

Austen L. Thompson[a], Shaness A. Grenald[a], Haley A. Ciccone[a], Dieter Mohty[a], Angela F. Smith[a], Deziree L. Coleman[a], Erfan Bahramnejad[a], Erick De Leon[b], Logan Kasper-Conella[b], Jennifer L. Uhrlab[c], David S. Margolis[b,d], Daniela Salvemini[e], Tally M. Largent-Milnes[a,f], Todd W. Vanderah[a,f,*]

Abstract

The propensity for breast cancer to metastasize to bone is coupled to the most common complaint among breast cancer patients: bone pain. Classically, this type of pain is treated using escalating doses of opioids, which lack long-term efficacy due to analgesic tolerance, opioid-induced hypersensitivity, and have recently been linked to enhanced bone loss. To date, the molecular mechanisms underlying these adverse effects have not been fully explored. Using an immunocompetent murine model of metastatic breast cancer, we demonstrated that sustained morphine infusion induced a significant increase in osteolysis and hypersensitivity within the ipsilateral femur through the activation of toll-like receptor-4 (TLR4). Pharmacological blockade with TAK242 (resatorvid) as well as the use of a TLR4 genetic knockout ameliorated the chronic morphine-induced osteolysis and hypersensitivity. Genetic MOR knockout did not mitigate chronic morphine hypersensitivity or bone loss. In vitro studies using RAW264.7 murine macrophages precursor cells demonstrated morphine-enhanced osteoclastogenesis that was inhibited by the TLR4 antagonist. Together, these data indicate that morphine induces osteolysis and hypersensitivity that are mediated, in part, through a TLR4 receptor mechanism.

Keywords: Opioids, Cancer-induced bone pain, Opioid-induced hypersensitivity, TLR4, Cancer pain, Breast cancer

1. Introduction

Cancers, including breast, prostate, and lung, have high affinity for metastatic spread to bone.[2] Cancer seeding and growth within bone leads to neuroinflammatory,[44,46,60] mechanosensory,[56] and bone homeostatic[52] dysregulation that contribute to the multimodal pain state of cancer-induced bone pain (CIBP). Cancer metastasis to bone promotes chronic pain and progressive osseous destruction increasing risk of pathological fracture and enhanced pain.[31] Cancer pain can be grouped into 2 categories: ongoing pain, which is chronic, and aching pain which worsens over time. Conversely, breakthrough pain characterized by sudden, severe pain that arises spontaneously or with movement or palpation.[5] Opioid-based analgesics are the gold standard for treating CIBP despite moderate-to-severe cancer pain is not adequately controlled using opioids in over 30% of patients.[64] Opioids have multiple adverse effects associated with sustained use including constipation, tolerance, respiratory depression, physical dependence, and hypersensitivity.[63,65]

Studies using a model of metastatic prostate cancer demonstrated decreased morphine hyperalgesia by the addition of an omega conotoxin, leconotide.[39] Recent reports suggest chronic morphine may exacerbate osteolysis accompanying sarcoma, which is counterproductive to antiresorptive drugs coadministered to assist with bone metabolism and pain.[37] Opioids ability to potentiate bone loss has been documented clinically in men,[17,23] women,[58] and the elderly.[59] Meta-analyses uncovered the association of opiate use and increased risk of fracture independent of age or gender.[61,67] Opioid use and fracture becomes increasingly problematic in cancer as skeletal health is closely correlated to quality of life and functional status, which are essential to decrease the high disease morbidity. Pathologic fracture in cancer patients portends higher mortality.[25,49,51] Preclinical and clinical studies show opioid use may enhance cancer progression, recurrence, and mortality,[3,4,20,31] although this is controversial and deserves more attention.

Preclinical evidence supports chronic morphine administration enhances tumor-induced bone loss and exacerbate pain

Sponsorships or competing interests that may be relevant to content are disclosed at the end of this article.

[a] Department of Medical Pharmacology, University of Arizona College of Medicine, Tucson, AZ, United States, [b] Department of Biomedical Engineering, University of Arizona, Tucson, AZ, United States, Departments of [c] Immunobiology and, [d] Orthopaedic Surgery, University of Arizona College of Medicine, Tucson, AZ, United States, [e] Department of Pharmacology and Physiology and Henry and Amelia Nasrallah Center for Neuroscience, Saint Louis University School of Medicine, St. Louis, MO, United States, [f] Comprehensive Pain and Addiction Center, University of Arizona, Tucson, AZ, United States

**Corresponding author. Address: University of Arizona, 1501 N Campbell Ave, Tucson, AZ 85725, United States. Tel.: (520) 626-7801. E-mail address: vanderah@email.arizona.edu (T. W. Vanderah).*

Supplemental digital content is available for this article. Direct URL citations appear in the printed text and are provided in the HTML and PDF versions of this article on the journal's Web site (www.painjournalonline.com).

http://dx.doi.org/10.1097/j.pain.0000000000002953

behaviors[37,66]; mechanisms underlying these are not well understood. Tumor presence within bone microenvironment enhances the influx of inflammatory cells and cytokines[31] that contribute to the multimodal pain phenotype. These proinflammatory factors promote osteoclast maturation and activation.[53]

The morphine metabolite, morphine-3-glucuronide, and other opioids produce off-target activation and downstream signaling of toll-like receptor-4 (TLR4).[18,27,30,69] Ellis et al. and Grace et al. separately demonstrated morphine activity on TLR4 potentiates spinal-mediated hyperalgesia in neuropathic pain. Toll-like receptor-4 signaling leads to the activation of nuclear factor kappa light-chain enhancer of activated B cells (NF-κB), a master regulator of inflammatory gene expression and cell differentiation. Nuclear factor kappa light-chain enhancer of activated B cells is a key regulator of osteoclast differentiation and activation, which can be mediated through inflammatory cytokines including interleukin 6 (IL-6) or through receptor activator of NF-κB ligand (RANKL).[53] TLR4 activation is upregulated within the tumor microenvironment in multiple metastatic cancer models, including breast, lung, and liver,[75] enhancing tumor progression through increased inflammation and recruitment of tumor-associated macrophages enhancing TLR4 expression.[15,75] We hypothesize chronic administration of morphine acts through TLR4 to promote osteoclastogenesis, osteolysis, and exacerbates hypersensitivity in a murine cancer-bone microenvironment.

2. Materials and methods

2.1. In vivo and ex vivo procedures

2.1.1. Animals

All studies used female C57BL/6J or BALB/c3H mice aged 7 to 9 weeks at the time of surgery (n = 10-14 animals per treatment group) for immunocompatability with the E0771 mammary adenocarcinoma or 66.1 mammary adenocarcinoma cell lines, respectively. Animals were obtained from Jackson Laboratories (Bar Harbor, ME). TLR4$^{-/-}$ (B6(Cg)-Tlr4<tm1.2Karp>/J, #029015) and MOR$^{-/-}$ (B6.129S2-Oprm1<tm1Kff>/J, #007559) mice were obtained from Jackson Laboratories (Bar Harbor, ME). Female mice were used based on the prevalence of breast cancer in females. All animals were maintained on a 12-hour light or dark cycle in a climate-controlled room and were provided access to food and water ad libitum. Animals were weighed on days 0 (day of surgery), 7, 10, and 14. Animals were all continually monitored for clinical signs of morbidity, including but not limited to infection, paralysis, rapid weight loss (>20% in 1 week), or full cortical fracture at which point the animal would be removed from the study. Additional criteria for study removal would be failure of surgery to induce pain at D7. Total numbers of animals used were as follows: wild type C57BL6/J—N = 80 (8 excluded due to surgical failure or failure to meet baseline measurements), TLR4$^{-/-}$—N = 24 (4 excluded due to surgical failure), and MOR$^{-/-}$—N = 24 (1 excluded due to surgical failure). Animals were randomly assigned groups, and all behavioral testing was performed using a blinded-to-treatment protocol.

2.1.2. Cancer-induced bone pain surgery

Intramedullary injections of E0771 cells were performed as previously described.[26,42,62,63] In brief, mice were anesthetized with ketamine/xylazine (9.0 mg/mL:1.0 mg/mL, i.p). A lateral incision was made on the right hind leg over the femur to expose the thigh muscle. An arthrotomy was performed, and the condyles of the distal femur were visualized. A hole was drilled in the intercondylar space to access the medullary cavity. 8×10^4 E0771 breast adenocarcinoma cells (P10-20) suspended in 5 μL volume of OPTI-MEM were injected into the medullary cavity using an injection cannula affixed by plastic tubing to a 10 μL Hamilton syringe; sham animals received only OPTI-MEM. Placement of the syringe within the intramedullary canal was confirmed using Faxitron x-ray imaging before injection of cells. After implantation, the hole in the distal femur was sealed using bone cement, arthrotomy was closed using 5-0 Vicryl suture, and the skin incision was closed using wound clips. Animals were allowed 7 days to recover before behavioral testing. Wound clips were removed 6 days after surgery under short volatile exposure of isoflurane anesthesia. Animals with radiographic signs of fracture before day 14 postsurgery were removed from the study, and their data were not included in analysis.

2.1.3. Spontaneous pain behaviors

Mice were placed individually into plexiglass chambers with a wire mesh floor and allowed to acclimate for 30 minutes before testing. Animals were observed for flinching and guarding behaviors over 2-minute periods as previously described.[42] In brief, flinching is characterized by the rapid flexing of the ipsilateral hind paw, whereas the animal was not moving and is counted by the number of flexing movements made. However, if the mouse shook its foot while walking, this was also counted as a flinch. Guarding is characterized by the animal holding the ipsilateral hind paw into a retracted position near or under the torso. Animals often will display either flinching or guarding at any given time, and outcomes should be observed as a combination of pain behaviors. Guarding behavior better represents on-going pain while flinching bouts may better represent spontaneous pain. All mice were baselined for these behaviors at day 0 before surgery. Pain baselines were obtained for all the animals at 7 days postoperative, before morphine or saline minipump implantation. Then animals were implanted with subcutaneous minipumps containing the appropriate dose of morphine or saline for continuous infusion. Animals were reexamined for pain behaviors at days 10 and 14 postsurgery. D10 and D14 behaviors were obtained with the minipumps in place. Behaviors were analyzed by treatment-blinded examiners who have been formally trained in scoring these behaviors in a standardized fashion. The same behaviorists were used for the entirety of the study to ensure reliability.

2.1.4. Radiographic analysis

Mice were anesthetized using isoflurane volatile anesthesia while being imaged using the digital Faxitron system (UltraFocus, Faxitron Bioptics, Tucson, AZ). Images were obtained on days 0 (before surgery), 7, 10, and 14 postsurgery and evaluated using a 5-point bone rating scale by 3 independent and blinded observers as previously described.[43,74] The bone scoring scale was as follows: 0 = normal bone; 1 = 1 to 3 lesions with no fracture; 2 = 4+ lesions with no fracture; 3 = unicortical, full-thickness fracture; and 4 = bicortical, full-thickness fracture. Animals with full cortical fracture before day 14 were euthanized, and their data were excluded from analysis.

2.1.5. Micro-computed tomography

After sacrifice, the experimental femora were explanted and scanned at 20 μm resolution using an Inveon micro-computed tomography (μCT) scanner (Siemens, Franklin Lakes, NJ) using

native software for analysis. The distal part of the femur, 5 mm proximal to the proximal border of the growth plate, was the region analyzed in each femur. The region of interest was selected on axial slices, oriented in the anterior–posterior and medial–lateral plane. The periosteal and endosteal surfaces of the femur were manually traced using the lasso tool every 5 slices with the intervening region of interest interpolated between the tracing. The region of interest occupied by methyl methacrylate was excluded. Trabecular bone assessment was performed by analyzing the region of interest within the endosteal cavity using threshold settings of min: 550/max: 1500 for bone. Cortical wall thickness was calculated as the average distance between the periosteal and endosteal surfaces. In total, bone volume/total volume (%), bone surface/bone volume (1/mm), trabecular thickness (μm), trabecular number (1/mm), trabecular spacing (μm), and cortical wall thickness (mm) values were obtained.

2.1.6. Preparation of femurs for flow cytometry

On day 14, mice were anesthetized, x-rayed, and sacrificed by cervical dislocation. Intact contralateral and ipsilateral femurs were collected, cleaned, and placed in microcentrifuge tubes containing cold Roswell Park Memorial Institute media. Individual femurs were then placed in fluorescence-activated cell sorting buffer and grinded with a ceramic pestle and mortar. The resulting suspension was strained through a 70 μm cell strainer 5 times to exclude bone fragments and other debris. The run-through collected into 50 mL tubes. All samples were then centrifuged at 2000 revolutions per minute for 5 minutes. After removing excess media, the pellets were resuspended using 200 μL fluorescence-activated cell sorting buffer (phosphate buffered saline with 2% FBS). 150 μL of each sample was transferred to a 96-well plate, with the remaining 50 μL allocated to create pooled samples for full-minus-one controls (FMOs).

2.1.7. Immunofluorescence staining and flow cytometry

Fifty microliter of Fc-Inhibitor solution (a 1:50 1 μL FC-block in 50 μL FACS buffer) was added to each sample to prevent nonspecific binding. The Fc-block incubated for 15 to 20 minutes. Thereafter, samples were stained for surface markers with 50 μL a prepared antibody solution. The solution was a 1:50 dilution of each antibody (CD3, CD11b, CD11c, CD19, CD115, CD117, CD206, NK1.1, F4/80, and CD265) in FACS buffer. Full-minus-one controls were created for the following antibodies: CD11c, CD68, CD115, CD117, CD206, and CD265. Samples were then allowed to incubate for 45 minutes at 4°C. Samples were then washed with 100 μL PBS and were then centrifuged for 3 minutes at 2000 RPM (Note: A "wash" step includes resuspension, centrifugation, and removal of excess media.) This wash was repeated with 100 μL PBS/well. After the second wash, each well was incubated with 100 μL solution of a 1:1000 dilution of Live-Dead viability dye. After another 30 to 45-minute incubation, the cells were washed with 100 μL PBS/well and then fixed with 200 μL/well of BD Cytofix solution. This was allowed to incubate for 5 to 7 minutes. Samples were then washed with 200 μL/well FACS buffer. After removing excess FACS media, a 100 μL of a 1:10 dilution perm-wash in dH_2O was added to each sample. The samples were then washed 3 times using 100 to 200 μL/well of perm wash. Cells were then stained intracellularly using a 1:50 dilution of CD68 in perm wash solution, with 50 μL pipetted per sample. After another 30 to 45-minute incubation, cells were washed with 100 μL and then 200 μL/sample of perm wash. After removing the excess media, a 1:5 dilution of count beads in FACS buffer (500 μL beads in 2000 μL FACS) was prepared. Each sample was resuspended using 50 μL of the count bead solution. Single color compensations were made using a 1:15 dilution of compensation beads (concentration of 10,500 beads/μL) in FACS buffer. For every antibody used, a microfuge tube containing 100 μL of the compensation bead solution was prepared. 1 μL of antibody was pipetted into its respective microfuge tube. We compensated Live-Dead using anti-human granzyme B (GzB) as it fluoresces in the same wavelength (PE TXR). This is because the compensation beads can only bind antibodies and the Live-Dead stain is not an antibody. For the triple negative channel (CD3/CD19/NK1.1 with A700 conjugation), 1 μL of each antibody was pipetted into a single microfuge tube. Rainbow beads were used before each run to verify laser and voltage consistency between runs. Data collection was standardized to the collection of 2500/5000 count beads, depending on the overall cell viability. All samples were stained and run through the LSRFortessa flow cytometer no more than 12 hours after sample preparation to maximize cell viability and antibody conjugation stability.

2.1.8. Flow cytometry gating protocols

See supplemental data for a representative gating protocol (see Supplemental Figure 1, demonstrating visual of flow cytometry gating protocol, available at http://links.lww.com/PAIN/B854). All data were collected and analyzed by FlowJoV2 software. Initial gating was performed by using the Live-Dead stain against the histogram. From the live proportion of cells, gating was performed against Side-Scatter (SSC-A) vs Forward-Scatter (FSC-A) using a wide range of sizes to attempt to encompass the large, mature osteoclast cells. Then, gating was performed on the agranulocyte populations against our triple-native gate of CD3/CD19/NK1.1; this allowed us to exclude T cells, B cells, and natural killer T cells, respectively. We then hypothesized that our cells of interest would be within this triple negative population.

2.1.8.1. MΦ and M1 macrophages

Triple negative cells from the preliminary analysis were then gated against F4/80 and CD11b, and the double-positive population was selected. $CD11b^{+}F4/80^{+}$ cells were then analyzed for markers to identify the polarization of cells. We could examine the MΦ, M1, and M2 macrophages using the immunophenotyping panel of CD11c, CD68, and CD206. We determined that $CD68^{+}$ cells were M1 macrophages. M2 macrophages were marked as $CD206^{+}CD11c^{-}$.

2.1.8.2. Myeloid cell lineage

We determined the population of cells that would contain osteoclast precursor (OCP) cells to be $CD11b^{-/low}$ expressing. We determined the population of cells that would contain late OCP cells were determined to be $CD11b^{mid/+}$ expressing. To accomplish this, we visualized the CD11b marker on a histogram by the intensity of fluorescence, which demonstrated 2 distinct peaks of fluorescence. These 2 distinct peaks allowed for determination of $CD11^{b-/low}$ and $CD11b^{mid/+}$ cells easily. Following this gating protocol, we could then stratify our final outcomes by CD115 and CD117 expression to determine early/late OCPs and osteoclasts (OC) cells more readily.

2.1.8.3. Early/late osteoclast precursor and osteoclasts cells

After the use of varied CD11b expression to dissect out the populations of cells where early OCPs, late OCPs, and OC cells may be found, we gated using the markers CD115 and CD117.

$CD115^+CD117^+$ cells were determined to be early OCPs. $CD115^+CD117^-$ cells were determined to be late OCPs.

2.1.8.4. Osteoclast cells

After determination of late OCPs, these populations were further gated against CD68 and CD265 (RANK). Cells that were $CD68^+RANK^+$ were interpreted to be mature osteoclasts.

2.1.9. Bone extrudate collection

This was a process adapted from previous studies.[54] Before the start of bone exudate collection, a stock solution of 1X PBS + 1X protease inhibitor cocktail was preloaded into 1 mL syringes (#309659, Becton Dickinson) with 25 to 5/8-gauge needles (305,122, Becton Dickinson) and placed on ice. Mice were then humanely euthanized under deep isoflurane anesthesia by cardiac puncture and rapid cervical dislocation. The femur was then dissected from the body using a 10-blade scalpel to cut through the acetabulum. The skin and muscle surrounding the femur was carefully removed using a 10-blade scalpel. The distal and proximal ends of the femur were then cut off to access the intramedullary space. Forceps were used to hold the femur over a 1.5 mL microcentrifuge tube, and the needle containing PBS + protease and phosphatase inhibitors was then inserted into the space. Marrow contents were forced through the femur and into the centrifuge tube. This process was repeated 6 times with the same 300 μL of solution to ensure complete flushing of each mouse femur. Three femurs per treatment group were pooled together in the same 300 μL of solution. The pooled contents were then homogenized by sonication and then centrifuged at 11,500 rpm for 5 minutes at 4°C. Supernatant was collected in fresh 1.5 mL tubes and stored at −80°C until used for analysis. Three to 5 separate pooled samples were evaluated from each treatment group representing a total of n = 9 to 15 animals.

2.1.10. Cytokine assay

Mice were sacrificed on postsurgical day 14 after behavioral testing. Femur extrudates were collected in the presence of a protease inhibitor cocktail (Prod # 78,430, Thermo Scientific, Rockford, IL) and stored at −80°C until ready for evaluation. A membrane-based antibody array (Proteome Profiler Mouse Cytokine Array Kit, Panel A; R&D systems) was used to detect the expression of 40 mouse cytokine and chemokines. Extrudate pools (n = 4 mice/pool) were thawed, and relative amount of protein was determined using the BCA protein assay (t# 23,225, ThermoFisher Scientific). Samples (200 μg) were mixed in a cocktail of biotinylated detection antibodies, placed on array membranes, and immersed in a cocktail of antibodies that bound specific target proteins. Chemiluminescence (#170-5061, Bio-Rad, Hercules, CA) was used to visualize the presence of mouse cytokines and chemokines. Relative expression was determined and quantified using Image J software.[57]

2.1.11. Pharmacological agents

Morphine sulfate was obtained from National Institutes of Health National Institute on Drug Abuse Drug Supply Program and was administered at a dose of 10 mg/kg/day. TAK242, specific TLR4 receptor antagonist, was obtained from Cayman Chemical (Cat #13871) and administered at a dose of 10 mg/kg/day, which is a dose that has been described in the literature in multiple models of disease.[19,72] Morphine was solubilized in saline vehicle. TAK242 was solubilized in a vehicle containing 10% dimethyl sulfoxide, 10% Tween-80, and 80% saline (vol/vol). Animals received one or a combination of various pharmacological agents from day 7 to 14 postsurgical inoculation with cancer cells. All drugs and vehicle treatments were administered by subcutaneous osmotic minipump (AZLET, Model 2001, 1.0 μL/hour for 7 days), and the use of dual subcutaneous minipumps[37] in mice has been previously described.

2.2. In vitro procedures

2.2.1. Cell culture

E0771 breast adenocarcinoma cells were grifted by Kathryn Visser at the Olivia Newton-John Cancer Research Institute Metastasis Research Institute (Victoria, Australia) and were used for immunocompatability with the C57BL/6J mouse strains. RAW264.7 murine macrophage cells were obtained from American Type Culture Collection (Manassas, VA). E0771 cells were maintained in Dulbecco modified Eagle medium (Mediatech, Manassas, VA) supplemented with 10% fetal bovine serum (vol/vol), 25 mM HEPES buffer, 100 IU^{-1} penicillin, and 100 μg/mL streptomycin. RAW264.7 cells were maintained in Dulbecco modified Eagle medium (Mediatech) supplemented with 10% fetal bovine serum, 100 IU^{-1} penicillin, and 100 μg/mL streptomycin. For additional proof of concept using a different murine breast cancer cell line, 66.1 breast adenocarcinoma cells (gifted by Dr. Amy Fuller),[68] were used for immunocompatability with the BALB/c3H syngeneic mouse line (Supplemental Figure 2, available at http://links.lww.com/PAIN/B854). 66.1 cells were maintained in α-Minimum Essential Medium (Mediatech) and supplemented with 10% fetal bovine serum (vol/vol), 100 IU^{-1} penicillin, and 100 μg/mL streptomycin. Cells were passaged every 4 days or as needed, and cells used for all experiments were in the 10 to 20 passage range.

2.2.2. Osteoclastogenesis assay

To study osteoclast-like differentiation, cells were seeded on a 96-well plate at a density of 104 cells per well. Cells were immediately treated with RANKL (1-100 ng/mL) or drug treatment for 5 to 7 days with media changes on every third day. Osteoclastogenesis was measured by observing the formation of multinucleated cells or by quantifying tartrate-resistant acid phosphatase (TRAP) in cell supernatant or on fixed cells using the K-assay TRAP staining kit according to manufacturer specifications (Kamiya Biomedical Company, Seattle, WA).

2.2.3. Immunocytochemistry and confocal microscopy

Bright field and laser confocal microscopy was conducted as previously described.[9] 66.1 tumor cells were seeded in 4-chamber slides (ThermoFisher Scientific) in regular growth media overnight. The next day, cells were treated with vehicle, morphine (10 μM), TAK242 (500 nM), or a combination of morphine and TAK242 (10 μM morphine + 500 nM TAK242) for 24 hours. Cells were then rinsed, fixed (with ice-cold ethanol), and permeabilized with Triton-X (Sigma, St. Louis, MO). Cells were blocked with 5% BSA in the presence of donkey serum for 1 hour at room temperature. Next, cells were allowed to incubate in NFκB phosphorylated-p65 primary (Cat# 3033, Cell Signaling, Beverly, MA), and secondary (#711-165-152, Jackson ImmunoResearch, West Grove, PA) antibodies before being cover slipped with prolong gold antifade reagent with DAPI (Life Technologies, Carlsbad, CA). Slides were allowed to dry overnight before imaging. Images of NFκB p-p65 expression were captured using an Olympus Bx51 microscope fitted with an Olympus Dp70 digital CCD camera and an UPlanSApo 10x/0.40 objective. The

Olympus Fluoview FV1000 (Olympus, Melville, NY) system contains Multiline Argon (458, 488, 515 nm), Green HeNe (543 nm), and Red HeNe (633 nm) lasers. In addition, the Olympus Fluoview FV1200 (Olympus) system (used for oil objectives) is equipped with LD (405, 440, 473, 559, 635 nm), Multiline Argon (457, 488, 515 nm), and HeNe(G) (534 nm) lasers. The Olympus Fluoview systems have multiple excitation and emission filters. NFκB phosphorylated-p65 and nuclear staining (DAPI) markers were visualized using excitation beams of 550 nm and 405 nm and emitted at 570 nm and 470 nm, respectively.

2.2.4. Pharmacological agents

Morphine sulfate, mu-opioid receptor agonist, was obtained from National Institutes of Health National Institute on Drug Abuse Drug Supply Program and was administered at a concentration of 10 μM. TAK242, the specific TLR4 receptor antagonist,[29,76] was obtained from Cayman Chemical (#13871) and administered at a concentration of 500 nM. Morphine was solubilized in normal or serum-free culture media vehicle. TAK242 was solubilized in 0.1% DMSO in cell culture media. Murine Receptor Activator of NFκB Ligand (RANKL) was obtained from Abcam (ab129136) and was solubilized in normal or serum-free culture media at concentrations ranging from 1 to 100 ng/mL. Cells were treated with one or a combination of these drugs for 24 hours before performing aforementioned assays.

2.2.5. Statistical analysis

All data were analyzed using either a 1-way ANOVA with Tukey post hoc correction or an ordinary repeated measure 2-way ANOVA with Bonferroni post hoc correction, depending on the experimental design. Nonparametric data sets were analyzed with the Kruskal–Wallis test, and multiple comparisons were made using the Dunn multiple comparisons test. Pairwise comparisons were made with the Student t test. For animal numbers, a power analysis was performed using GPower3.1 software and we found adequate statistical separation for each group to detect 0.80 between groups at $P < 0.05$. Data were expressed as mean ± standard deviation or standard error of the mean with all analysis being performed using GraphPad Prism 7.0 (GraphPad Inc, San Diego, CA) or using SPSS Statistics (IBM Inc, Chicago, IL). Studies were all performed with treatment blinded observers.

2.2.6. Study approval

All animal procedures were approved by the University of Arizona Animal Care and Use Committee (06-110/19-600) and conformed to the Guidelines for the Care and Use of Laboratory Animals of the National Institutes of Health and the International Association for the Study of Pain.

3. Results

3.1. Chronic morphine treatment induces hypersensitivity in a cancer-induced bone pain model

To study the effects of morphine treatment on bone-derived pain from metastatic breast cancer, we used an established and previously published model that reliably replicates long bone pain due to cancer.[43,62] In our syngeneic model, the E0771 breast adenocarcinoma cell line or media control (sham) were injected into the medullary canal of healthy female C57BL/6J mice and allowed to seed the site for 7 days. On day 7 postsurgery, flinching and guarding behaviors were observed and recorded over 2 minutes to obtain a postcancer baseline. Immediately after baseline, subcutaneous osmotic minipumps were implanted to deliver 10 mg/kg/day morphine sulfate or saline vehicle for the next 7 days. Flinching and guarding behaviors were then monitored on days 10 and day 14 after CIBP surgery to ascertain antihypersensitivity. On day 7, a significant increase in flinching behavior was observed in the mice seeded with cancer compared with the sham groups. Before treatments of morphine or saline, animals were divided into 4 groups and day 7 thresholds were measured. The cancer–morphine and cancer–saline groups had significantly higher flinching values compared with sham–morphine and sham–saline (7.5 and 8.75 vs 2.7 and 2.17, $P < 0.001$, **Fig. 1A**). On day 10, the cancer inoculated animals treated with morphine had significantly reduced flinching behaviors compared with the cancer-saline group (3.54 vs 7.42, $P = 0.0009$, **Fig. 1A**) demonstrating an antinociceptive effect. On day 14, morphine was no longer antinociceptive in cancer inoculated mice exhibiting tolerance or morphine-induced hypersensitivity with flinching increased over cancer inoculated mice receiving saline (10.00 vs 8.5, $P < 0.001$, **Fig. 1A**). There was a significant increase in flinching behaviors for the cancer-morphine group compared with both sham-morphine and sham-saline groups (10.00 vs 2.8 vs 3.00, $P < 0.0001$, **Fig. 1A**). No significant difference in guarding values was observed until D14 at which point, the animals treated with morphine demonstrated markedly elevated amount of guarding compared with cancer–saline treated alone, further confirming morphine-induced hypersensitivity (2.06 vs 0.60, $P < 0.0001$, **Fig. 1B**). Sham–morphine, sham–saline, and cancer–saline had no significant differences in guarding behaviors at D14 (**Fig. 1B**). To enhance reproducibility, identical experiments were performed in an alternate mouse strain (BALB/c3H) with another syngeneic breast adenocarcinoma cell line (66.1) with similar results of morphine-enhancing pain behaviors by day 14 ($P < 0.001$) and attenuation by the TLR4 antagonist TAK 242 ($P < 0.0001$), suggesting a translatable model (see Supplemental Figure 2, demonstrating similar findings in separate model, available at http://links.lww.com/PAIN/B854).

3.2. Chronic morphine treatment significantly exacerbates cancer-induced osteolysis

Concurrent to monitoring the analgesic effects of chronic morphine on these animals, the disease progression was monitored in vivo using radiography. To evaluate the effects of morphine on tumor-related bone loss, radiographs were obtained at baseline (before surgery), day 7, 10, and 14 after inoculation. Animals were then compared at day 14 to assess osteolysis using a previously described 5-point bone rating scale.[43,74] Animals inoculated with cancer cells had significantly elevated bone scores compared with sham inoculated controls, regardless of their treatment (2.7/3.46 vs 0.75/0.67, $P < 0.0001$, **Figs. 2A and B**) indicative of cancer-induced bone loss. Between the cancer groups, the animals treated with morphine displayed a further elevated bone score, which indicates that morphine treatment enhanced the tumor-induced osteolysis compared with animals treated with saline alone (3.46 vs 2.70, $P < 0.0001$, **Figs. 2A and B**).

After seeing the dramatic radiographic differences in cancer animals treated with morphine compared with those receiving saline alone, we further quantified these findings using micro-computed tomography (μCT). Analysis revealed that cancer animals treated with morphine had decreased bone volume/total volume (BV/TV, %) ratio (15.8 vs 23.4, $P < 0.05$), trabecular number (TN, 1/mm) (4.1 vs 5.8, $P < 0.05$), and cortical wall thickness (mm) (0.13 vs 0.16, $P < 0.005$) (**Table 1**). In addition, the animals treated with morphine had minimal reactive bone

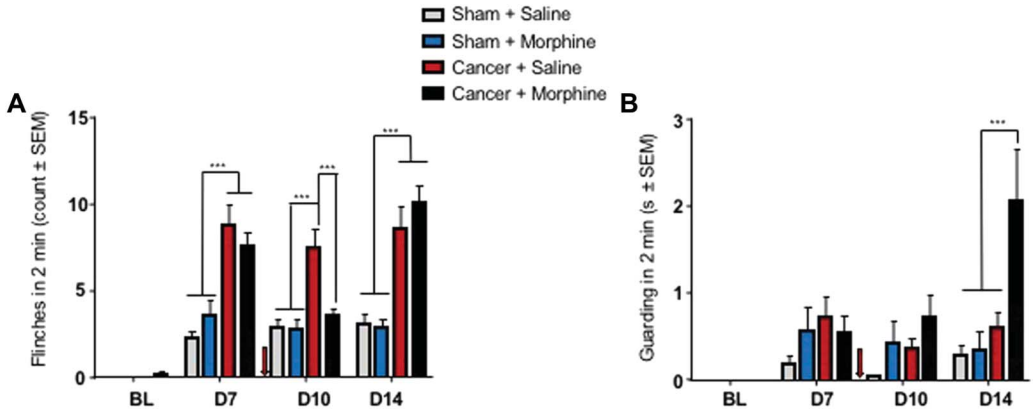

Figure 1. Chronic morphine treatment leads to hypersensitivity in murine model of cancer-induced bone pain. Spontaneous pain behaviors (flinching and guarding) were measured before and at regular intervals after cancer inoculation in female C57BL/6J mice. (A) At D7 postsurgery, animals inoculated with E0771 breast adenocarcinoma cells had significantly elevated flinching behaviors compared with sham animals. At D10, after treatment, morphine-treated cancer animals had significantly reduced flinching compared with saline-treated cancer animals; cancer–morphine animals had similar flinching behaviors as sham controls. At D14, cancer-morphine–treated animals had significantly elevated flinching behaviors compared with D10 and compared with sham controls, indicating antinociceptive tolerance or morphine-induced hypersensitivity. Interaction $F(9,172) = 6.976$, $P < 0.0001$. (B) No significant guarding behavior was observed until D14 postsurgery, which showed cancer inoculated animals treated with morphine demonstrated significantly elevated amounts of guarding compared with cancer inoculated sham-treated animals as well as sham animals. Interaction $F(9, 176) = 3.136$, $P = 0.0016$. Red arrows indicated the start of drug treatments. Data are expressed as means ± SEM. ***$P < 0.001$, n = 11 to 13/treatment (2 way repeated measures ANOVA, Bonferroni post hoc).

formation and multiple displaced fractures compared with the cancer-alone group, which had evidence of periosteal reaction to the lytic lesions (see Supplemental Figure 3, representative micro-CT images, available at http://links.lww.com/PAIN/B854).

To determine if bone loss resulted from a decrease in osteoblasts, increase in mature osteoclasts, or a mixed model, flow cytometry was performed on the inoculated femurs to determine changes in osteoclast cell lineages. Mature OC, to date, have not been reliably sorted using published flow cytometric methods, but their direct OCPs have been successfully sorted. Using an antibody panel that was adapted from previously described methods to identify OCPs,[50,73] animals with cancer had significantly elevated amounts of OCP within the ipsilateral bone when compared with naïve and sham animals. Although not achieving statistical significance, animals treated with morphine had a trend towards increased frequency of these cells (**Fig. 2C**). With additional gating schemes, we looked at the populations of $CD11b^{-/low}$, which will decrease as OCPs mature into osteoclasts, indicating increased amount of CD11b expression in animals with cancer compared with naïve and sham animals (**Fig. 2D**).

3.3. Toll like receptor-4 pharmacological antagonism leads to loss of morphine-induced hypersensitivity and attenuated morphine-induced osteolysis

To further elucidate the receptor mechanisms underlying morphine-induced hypersensitivity, we chronically coadministered morphine and the TLR4-specific antagonist, TAK242,[19,72] from day 7 to 14 postsurgical cancer inoculation. We collected spontaneous pain behavioral measurements at days 7, 10, and 14 to establish if analgesia is maintained. There was no significant difference in flinching behaviors at D7 between the groups. On day 10, morphine exhibited normal analgesic efficacy in the presence and absences of TAK242 (3.30 vs 3.54, $P > 0.999$, **Fig. 3A**) while saline in the cancer inoculated animals in the absence or presence of TAK242 alone resulted in a significant number of flinches on day 10 (7.80 vs 7.41, $P < 0.01$, **Fig. 3A**). On day 14, animals treated with morphine/TAK242 had significantly reduced amount of flinching compared with morphine-only treated animals (5.10 vs 10.00, $P = 0.003$, **Fig. 3A**). TAK242 alone had no significant effect on lowering or exacerbating flinching or guarding behaviors when compared with either morphine (1.67 vs 2.06, $P = 0.47$, **Fig. 3B**) or saline-treated animals (1.67 vs 0.601, $P = 0.601$, **Fig. 3B**). These data suggest that morphine-induced hypersensitivity in our CIBP model is regulated, in part, by a TLR4-mediated mechanism.

To evaluate the effect of morphine on bone tumor–related bone loss was mediated by TLR4, radiographs of the ipsilateral femur from these mice were taken for analysis at 0 and 14 days postsurgery (dps) (**Fig. 4A**). On day 14, after 7-day drug treatment, morphine-treated mice demonstrated a greater degree of bone loss than cancer-inoculated vehicle controls; however, bone loss in morphine/TAK242-treated mice was indistinguishable from cancer-inoculated vehicle controls suggesting the blockade of TLR4 attenuated the morphine-induced osteolysis (**Fig. 4B**). TAK242 alone had no effect on bone integrity. These data suggest that morphine-induced bone loss that occurs in the E0771-C57BL/6J model is mediated, in part, by a TLR4-dependent mechanism.

3.4. Hypersensitivity is blunted in toll-like receptor-4 deficient mice but not MOR deficient mice

To confirm our pharmacological antagonist findings, we examined if germline, genetic knockout of TLR could recapitulate the findings that were observed in the antagonist studies. Using $Tlr4^{<tm1.2Karp>}$ knockout mice, a global TLR4 deficient mouse obtained from Jackson Laboratories, we performed the experimental protocol identical to the wild type studies. We tested spontaneous pain behaviors at days 0 (baseline), 7 (pretreatment), and 10 and 14 before sacrificing. Morphine reduction of flinching and guarding was similar to that of wildtype at day 10 (**Fig. 5A**) in TLR4 knockout mice. On day 14, morphine-induced antinociception was maintained and both flinching and guarding behaviors were significantly lower than wild-type animals treated with morphine (**Figs. 5A and B**).

We then performed the same experiments using a global mu-opioid receptor deficient mice, $Oprm1^{<tm1Kff>}$. In this animal, no significant difference was observed in flinching or guarding behaviors across the time course between knockouts and wild-type animals (**Figs. 5C and D**). These data taken together, along

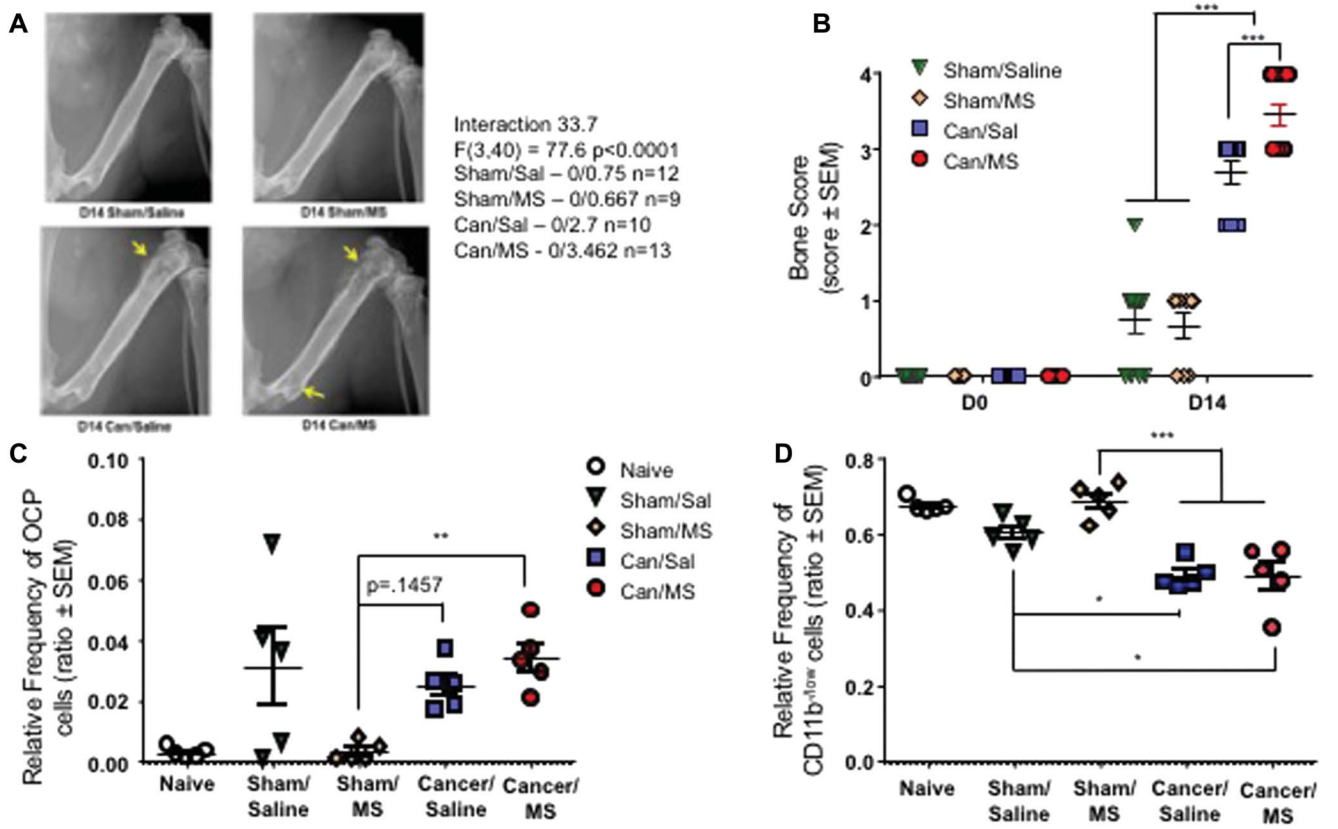

Figure 2. Chronic morphine treatment leads to enhanced osteolysis as evidenced by radiograph in mouse models of CIBP. (A) Representative radiographs of right femur of mouse D14 postsurgery. Plain radiographs were obtained before surgery and at D14 postsurgery to monitor cancer-induced lesion. (B) Quantification of bone scores (n = 9-13/treatment). Bones scores were determined on a 5-point scale by blinded observers. The scoring system was as follows: 0 = normal bone, 1 = 1 to 3 lesions with no fracture, 2 = 4+ lesions with no fracture, 3 = unicortical, full-thickness fracture, and 4 = bicortical, full-thickness fracture. (C) Contents of the marrow cavity were obtained on sacrifice, and cells were collected for flow cytometry. Relative OCP frequency was determined across the groups demonstrating the morphine-treated cancer inoculated animals had a significantly higher amount of OCP cells compared with sham and naïve animals (n = 5/treatment). (D) Cancer-treated animals had a significantly lower frequency of $CD11b^{-/low}$ cells within the ipsilateral bone, which is indicative of cellular differentiation toward macrophage/dendritic cell/osteoclast cell line (n = 5/treatment). ANOVA F(3, 40) = 77.61, $P < 0.0001$. Data are expressed as means ± SEM. $^{*}P < 0.05$, $^{**}P < 0.01$, $^{***}P < 0.001$ (one-way ANOVA, Tukey HSD post hoc). Can-MS, can–morphine; Can-Sal, can–saline; CIBP, cancer-induced bone pain; OCP, osteoclast precursors.

with the pharmacological antagonist studies, indicate that TLR4 plays a role in mediating opioid-induced hypersensitivity in cancer-induced bone pain.

3.5. Morphine-induced osteolysis in cancer-induced bone pain models is attenuated in toll-like receptor-4 but not MOR deficient mice

We next evaluated breast cancer-induced bone loss for the $TLR4^{-/-}$ and $MOR^{-/-}$ animals after morphine infusion and compared these with wild-type control animals. In the $TLR4^{-/-}$ mice, significant differences in bone scores were not observed between the morphine-treated and the vehicle-treated cancer animals, whereas morphine significantly lowered bone scores in the wild type cancer or morphine-treated animals beyond those of cancer–vehicle (**Figs. 6A and B**). In the $MOR^{-/-}$ mice, although trending, there was no significant difference in bone scores between the wild-type cancer morphine and the $MOR^{-/-}$ morphine ($P = 0.08$, **Figs. 6A and B**). These data support TLR4, but not MOR, as necessary for morphine-induced osteolysis.

3.6. Morphine enhances expression of proinflammatory cytokines and upstream and downstream regulators of toll-like receptor-4 in the murine model of cancer-induced bone pain

NF-κB is a well-described downstream target of the TLR4 receptor.[35,36] We, therefore, investigated how the expression of

Table 1

Objective bone microcomputed tomography measurements of animals inoculated with cancer-treated with saline or morphine.

Tables: Groups	Bone volume/total volume (%)	Bone surface/bone volume (1/mm)	Trabecular thickness (μm)	Trabecular number (1/mm)	Trabecular spacing (μm)	Cortical wall thickness (mm)
Sham control	22.2 ± 1.7	53.4 ± 2.1	37.5 ± 1.5	5.9 ± 0.2	131.7 ± 7.8	0.17 ± 0.01
Can-Sal	23.4 ± 6.1	50.4 ± 4.5	40.0 ± 3.8	5.8 ± 0.9	135.8 ± 28.7	0.16 ± 0.01
Can-MS	15.8 ± 4.3*	52.8 ± 3.1	38.0 ± 2.2	4.1 ± 1.1*	219.3 ± 78.3	0.13 ± 0.02†

* $P < 0.05$ for Can-MS vs control and Can-Sal.
† $P \leq 0.005$ for Can-MS vs control and Can-Sal.
Can-MS, can-morphine; Can-Sal, can-saline.

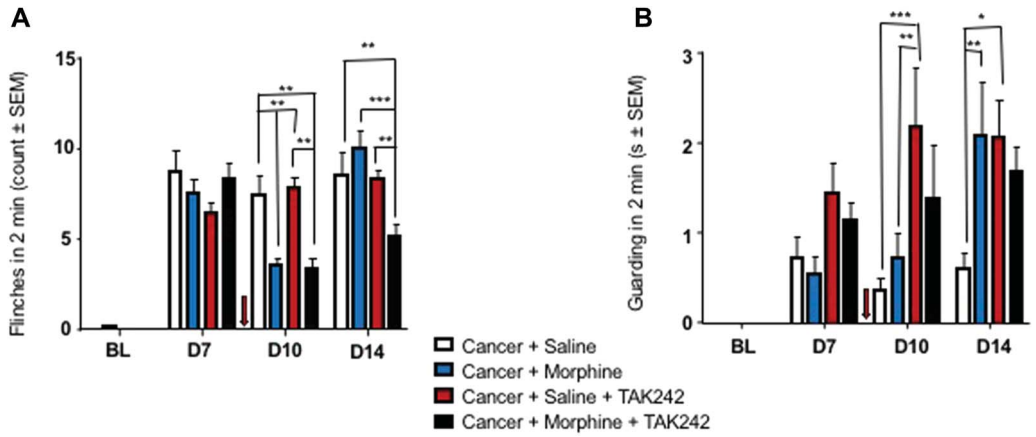

Figure 3. Pharmacological inhibition of TLR4 leads to blunting of hypersensitivity and maintained efficacy of morphine-induced anti-nociception in CIBP. Spontaneous pain behaviors (flinching and guarding) were measured before and at regular intervals after cancer inoculation in female C57BL/6J mice. (A) At D7, all groups developed similar levels of flinching before treatment initiation. At D10, morphine administration significantly lowered flinching behavior compared with saline control regardless of TLR4 inhibition. At D14, TLR4 inhibition when coadministered with morphine maintained analgesic efficacy and significantly reduced flinching behaviors compared with all other groups. Interaction $F(9, 123) = 5.328$, $P < 0.0001$. (B) At D7, no significant difference in guarding behaviors was observed between groups. At D10, treatment with TAK242 alone had no effect on guarding behavior and was significantly elevated compared with cancer–saline and cancer–morphine alone. At D14, TAK242 and morphine was not significantly different from any of the other groups but was trending lower than cancer–morphine or cancer–TAK242 alone. Red arrows indicate the start of treatment. Interaction $F(9, 123) = 2.146$ $P = 0.0304$. Data are expressed as means ± SEM. $^*P < 0.05$, $^{**}P < 0.01$, $^{***}P < 0.001$ n = 10 to 12/treatment. (Two-way repeated measures ANOVA, Bonferroni post hoc). CIBP, cancer-induced bone pain; TLR4, toll-like receptor-4.

inflammatory cytokines was altered in the medullary cavity of CIBP mice treated with morphine. Using a dot blot assay, relative expression of the various cytokines was analyzed. It was found that, compared with cancer animals treated with saline alone, animals treated with morphine has a robust increase in the relative amount of various screened cytokines as well as the overall number of unique, inflammatory markers (**Table 2**). Of particular interest, M-CSF, C5a, and IL-16 all increased in cancer-MS groups relative to the cancer–saline group, which are known downstream regulators of NF-κB expression and activation.[35]

3.7. Morphine enhances osteoclastogenesis in vitro in a toll-like receptor-4–dependent manner

Next, we assessed the ability of morphine to facilitate osteoclastogenesis in vitro through a TLR4-dependent mechanism using an osteoclast precursor cell. Cultured RAW264.7 murine macrophages[55] were treated with RANKL (20 ng/mL) in the presence or absence of morphine (30 μM) or TAK242 (500 nM) in the media for 7 days to allow osteoclast differentiation process to occur (**Fig. 7A**). Levels of tartrate-resistant acid phosphatase (TRAP), a marker for osteoclast maturation,[55] were measured in

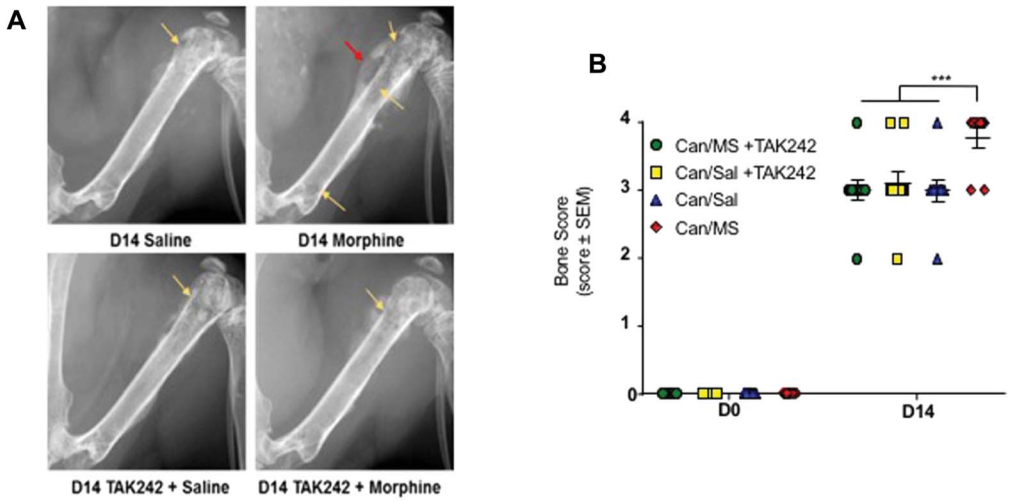

Figure 4. TLR4 inhibition reduces morphine-induced osteolysis in CIBP. (A) Representative radiographs of right femur of mouse D14 postcancer inoculation surgery in all animal groups. Increased bone degradation was observed in the morphine only treated groups as compared with the saline, TAK242 only, and the morphine-TAK242 cotreated groups. (B) Quantification of bone scoring in response to TLR4 inhibition by TAK242. There was no significant difference between the morphine/TAK242, saline/TAK242, or saline-alone treated cancer inoculated animals (3.00 vs 3.10 vs 3.00, $P = 0.999$, n = 9-10/group). TAK242 with morphine cotreatment demonstrated a significantly lower bone score when compared with the morphine treated alone, (3.00 vs 3.78, respectively, $P = 0.001$, n = 9-10/group). Yellow arrows = areas of osteolysis and bone degeneration, red arrows = areas of aberrant osteoblastic activity. Data represented as mean score ± SEM. Interaction $F(3,34) = 5.174$, $P = 0.0047$ n = 9 to 10/treatment. $^*P < 0.05$, $^{**}P < 0.01$ $^{***}P < 0.001$. (Two-way RM ANOVA, Bonferroni post hoc). Can-MS, can-morphine; Can-Sal, can-saline; CIBP, cancer-induced bone pain; TLR4, toll-like receptor-4.

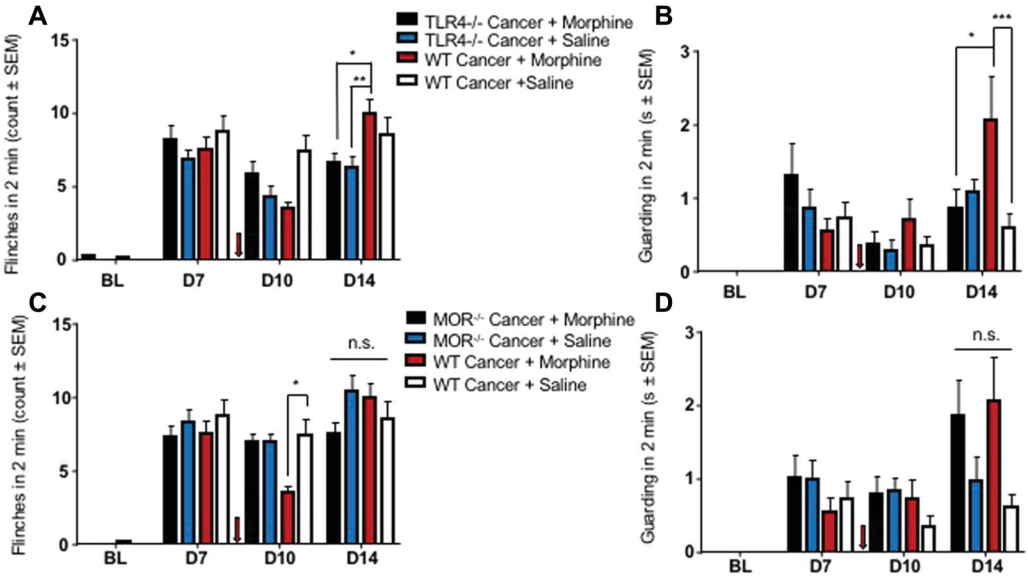

Figure 5. TLR4$^{-/-}$ mice inoculated with cancer have blunted hypersensitive responses to morphine and maintain morphine-induced antinociception. Genetic deletion of TLR4, but not MOR, attenuates morphine-induced hypersensitivity seen on day 14, resulting in maintained morphine analgesic efficacy. (A) Flinching behaviors were recorded for the various groups at days 7, 10, and 14 postcancer inoculation in all groups. At D14, it was observed that in the TLR4$^{-/-}$ mice had a significant reduction in flinching behaviors when compared with the wild-type mice treated with morphine (TLR4/MS: 6.58 vs WT/MS: 10.00 flinches, $P = 0.013$). (B) Guarding behaviors were also recorded in these groups and similarly demonstrated a significant reduction in guarding behavior at D14 in the TLR4/MS group compared with the WT/MS group (0.864 vs 2.06, $P = 0.02$). (C) Similar studies were performed in MOR$^{-/-}$ mice. At D14, there was no significant difference in flinching behavior between the knockout animals and the wild types, regardless of treatment. (D) Guarding behavior was also monitored, and similar to the flinching behaviors, there was no significant difference in the behaviors at D14 ($F[9,176] = 1.733$, $P = 0.085$). All data represented as mean ± SEM. $^{*}P < 0.05$, $^{**}P < 0.01$ $^{***}P < 0.001$, n = 12 to 13/group (two-way repeated measures ANOVA, Bonferroni post hoc). TLR4, toll-like receptor-4; wild-type cancer/morphine (WT/MS).

conditioned media and/or stained on fixed cells on the seventh day. Red and multinucleated (≥3 nuclei) cells were considered as differentiated osteoclast-like cells. The number of TRAP + cells was counted blindly by 2 persons.[10] RANKL treatments resulted in a significant increase in TRAP staining as compared with vehicle ($P < 0.05$) or morphine alone. Yet, RANKL and morphine-stimulated cells showed an even further significant increases in TRAP activity over vehicle and RANKL alone treatments ($P < 0.0001$). This effect was completely blocked by the TLR4 antagonist, TAK242 ($P < 0.0001$), suggesting morphine works through a TLR4-mediated mechanism to promote osteoclastogenesis (**Fig. 7B**).

4. Discussion

Cancer-induced bone pain is a notoriously difficult pain to manage clinically and has high associated morbidity. Currently, the World Health Organization provides a 3-step analgesic ladder strategy for advising the pharmacological management of these patients, with opioids being used on steps 2 and 3.[6] To achieve adequate pain relief, patients seek to maintain a steady-state plasma level of the analgesics to prevent chronic, dull pain, combined with oral administration to combat the associated breakthrough pain.[24,48,70] In this study, we have developed a preclinical model of metastatic breast cancer to bone that allows us to assess both spontaneous and ongoing pain phenotypes in a syngeneic model on a C57Blk/6J background to facilitate use of knockout lines and accounts for the role of the host immune system in disease and pain progression. In addition, we have accurately modeled the clinical pharmacological system by treating with subcutaneous osmotic minipumps, which allows for constant serum levels of the tested pharmacological drugs. For the first time, we demonstrate that continuous morphine treatment in a murine metastatic breast adenocarcinoma model induces hypersensitivity and enhanced osteolysis that is attenuated with the use of a selective TLR4 antagonists, as well as in genetic TLR4 knockout mice, which was not observed in mu-opioid receptor knockout mice.

Opioid-induced bone loss has been suggested and demonstrated in both preclinical and human populations; but to date, there have been no conclusive mechanisms suggested as to how this may occur. Overwhelmingly, it has been alluded that chronic opioid use induces a measurable endocrinopathy that may play a role in the reduced bone mass seen in both preclinical and clinical settings.[16] It is known that MOR activation in the hypothalamus will inhibit gonadotropin-releasing hormone (GnRH) thus leading to decreased androgen production and a condition known as opioid-induced androgen deficiency.[12] Although this may, and likely does, play a role in the development of opioid-induced bone loss, a recent report indicates that this effect may be independent of the antiandrogen effects of opioids[11] suggesting there may be additional mechanisms. Furthermore, observation does not account for the observed effects of opioid-induced osteoclastogenesis and enhanced osteolysis as evidenced by plain radiograph, μCT in our model of CIBP as well as the robust enhanced osteoclastogenesis seen in precursor macrophages in vitro.

Morphine and other mu-opioid agonists can activate TLR4.[27] TLR4 has a unique receptor pharmacologically because of its role as a pattern recognition receptor (PRR), which complicates traditional binding studies. Its role as a PRP may explain why morphine and other nonendogenous opioid agonists, which are structurally distinct from endogenous opioid agonists, are able to activate the receptor. Evolutionarily, the TLRs evolved to recognize foreign molecular structures and induce an innate inflammatory response.[36] Initial work in morphine-TLR4 interactions demonstrated that opioids bind to and facilitate TLR4 activation through the binding of the MD2 accessory protein,[28]

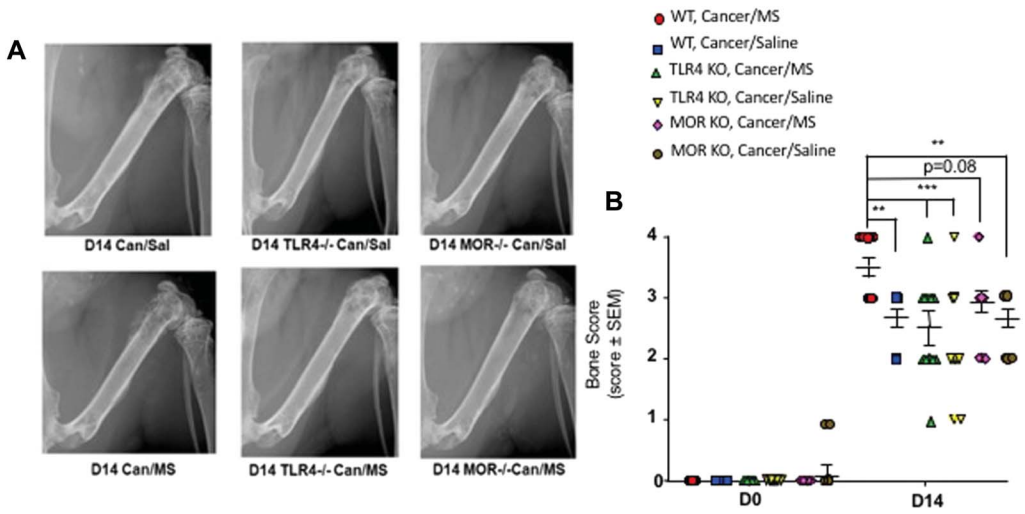

Figure 6. Genetic deletion of TLR4, but not MOR, attenuates morphine-induced osteolysis in a murine model of CIBP. (A) Representative radiographs are presented to demonstrate the effects on cancer on bone integrity at D14 postcancer inoculation. (B) Quantification and comparison of bone scores at D14 postcancer inoculation. Wild-type cancer/morphine (WT/MS)-treated animals had a significantly higher bone score at D14 compared with WT/Sal, TLR4KO/MS, TLR4KO/Sal, or MORKO/Sal groups (3.46 vs 2.70 vs 2.58 vs 2.42 vs 2.64, respectively, $P < 0.01$). MORKO/MS group did not have a significantly different bone score compared with WT/MS (2.92 vs 3.46, $P = 0.08$). All data represented as mean ± SEM. Interaction $F(5, 64) = 3.961$ $P = 0.0034$, n = 10 to 12/group. $^{**}P < 0.01$, $^{***}P < 0.001$ (2-way repeated measures ANOVA, Bonferroni post hoc). CIBP, cancer-induced bone pain; MS, morphine; Sal, saline; TLR4, toll-like receptor-4.

which caused downstream signaling as well as increased TLR4 transcription, translation, and trafficking.[69] TLR4 activation leads to downstream activation of the NF-κB pathway the activation of this pathway not only has been demonstrated to increase tumor growth[41] and increase inflammation within the tumor microenvironment[34] but tangentially promotes osteoclastogenesis while simultaneously inhibiting osteoblast maturation.[8,40] In our study, we noticed that, compared with cancer animals treated with saline alone, animals receiving chronic morphine had increased relative expression of various proinflammatory cytokines such as C5a, IL-16, and M-CSF. These have been shown previously to be strong activators of NF-κB as well as downstream products of NFκB activation.[35] In addition, we used data-mining software to predict transcription fact–gene promotor interactions between the selected cytokines, which predicts that NFκB can act to enhance transcription of various cytokines that were found to be upregulated, namely, C5a and M-CSF (**Table 3**). It can be inferred that the activation of NF-κB through this TLR4-mediated pathway can cause a positive feedback system to promote further inflammation within the bone tumor microenvironment, possibly worsening osteoclastogenesis and osteolysis.[1,53] Taken together, this creates a plausible mechanism by which morphine and other opioids may act in CIBP to enhance osteolysis: tumor presence within the medullary cavity increases TLR4 expression within the microenvironment by immune cell influx[15,75]; therefore, opioids have increased chance to interact with the receptor and induce inflammatory cytokines expression and downstream transcription factors that promote osteoclastogenesis—leading to enhanced osteolysis. Of note, morphine alone, without preceding insult to the bone and inflammation, did not cause radiologically evident bone loss.

To further characterize the effects of morphine on osteoclastic differentiation, we sought out an in vitro model. We demonstrated that the incubation of RAW264.7 cells, precursor cells to osteoclasts, in the presence of RANKL and morphine had significantly elevated TRAP activity compared with RANKL alone; this effect was completely abolished with TAK242 treatment. Morphine alone had no effect on osteoclast differentiation. This supports the hypothesis that the effects seen within this model are not due to systemic inflammatory responses but rather a localized

Table 2

Expression of key cytokine and chemokines in D14 marrow.

Cytokine	Can-saline	Can-morphine
CXCL13/BLC/BCA-1		+
C5a	+	++
G-CSF		+
ICAM-1		+
IFN-γ		+
IL-1β		+
IL-1ra	++	++
IL-16	+	++
IL-17		+
IL-23		+
CXCL10/IP-10		+
CXCL1/KC		+
M-CSF	++	++
CCL2/JE/MCP-1	++	++
CXCL9/MIG		+
CCL3/MIP-1α	+	+
CXCL2/MIP-2		++
CCL5/RANTES		+
CXCL12/SDF-1		+
TIMP-1	++	++
TNF-α	+	++
TREM-1	+	++

After completion of behavioral studies, animals were sacrificed. Harvested marrow samples were analyzed for relative expression levels of cytokine/chemokines from mouse array ELISA.
+, low expression levels; ++, high expression levels.

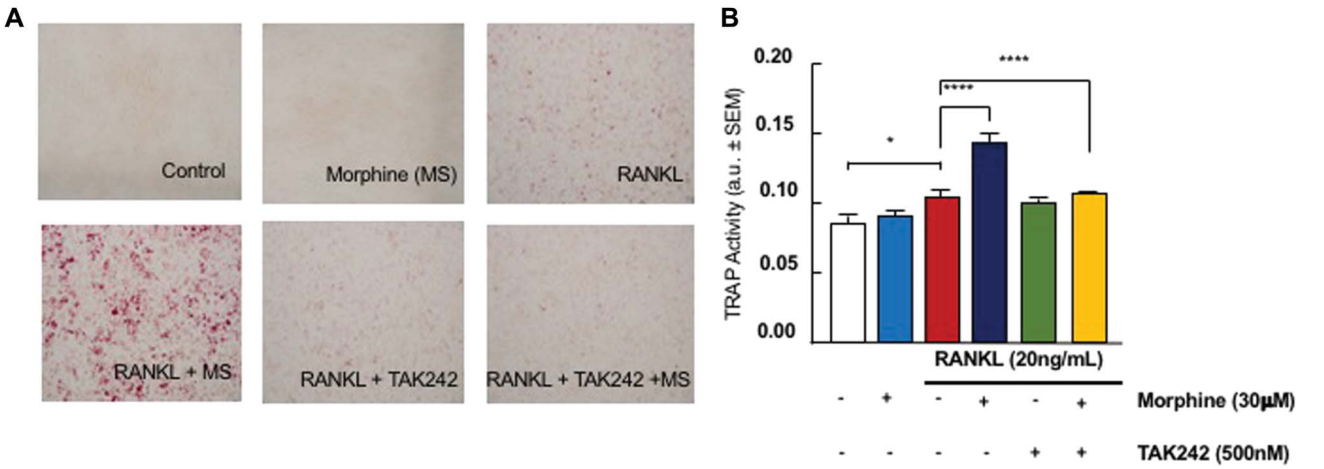

Figure 7. TLR4 receptor inhibition prevents morphine-enhanced osteoclastogenesis of RAW264.7. (A) RAW264.7 cells were treated with RANKL (20 ng/mL) in the presence or absence of morphine (30 μM) or the TLR4 antagonist, TAK242 (500 nM) for 7 days to allow for differentiation and then stained for tartrate resistant acid phosphatase (TRAP). Representative images are displayed (×10). (B) Quantification of TRAP activity in conditioned media. Data are expressed as means ± SEM. One-way ANOVA, Tukey post hoc correction. (*$P < 0.05$, ****$P < 0.0001$. n = 4 cultures/condition). TLR4, toll-like receptor-4.

inflammation within the bone-tumor microenvironment. It has been previously demonstrated that tumor and tumor-associated stromal cells can release osteoclast promoting factors such as RANKL and SOST.[53] Recently, it has also been demonstrated that the TLR4 signaling pathway can increase osteoclastogenesis in a RANKL independent manner, which further explained how pathways may interact to promote osteolysis.[1] Morphine, in the presence of enhanced osteoclast differentiation, microenvironments as we modeled in vitro and in vivo, exacerbates the differentiation response in a TLR4-dependent mechanism. We have summarized the probable impact of chronic morphine administration's activity on TLR4 receptor thereby leading to expression of proinflammatory

Table 3

Transcription factors that regulate multiple cytokines of interest in the marrow of chronic morphine-treated mice.

Transcription factor	C5/C5a	IL-16	M-CSF	CCL2	CXCL12	TIMP-1	TREM-1
NCX		++					
RP58		++					
USF1:USF2		++					
USF1		++					
USF2		++					
SEF1		++					
Evi-1		++					
ARP1				++			
LUN1				++			
POU3F2				++			
NFKB	++		++	++			
NFKB1	++		++	++			
RelA			++	++			
Pax4a				++			++
NFKB2			++	++	++		
Zic2					++		
NRSF1					++		
NRSF2					++		
Zic1					++		
FOXC1					++		
ITF2					++		
Tal1β					++		

Data represent the most relevant transcription factor binding sites in this gene promoter as predicted by SABiosciences' Text Mining Application.
++, Major transcription factors reported to regulate expression of gene; +, other transcription factor sites identified in UTR.

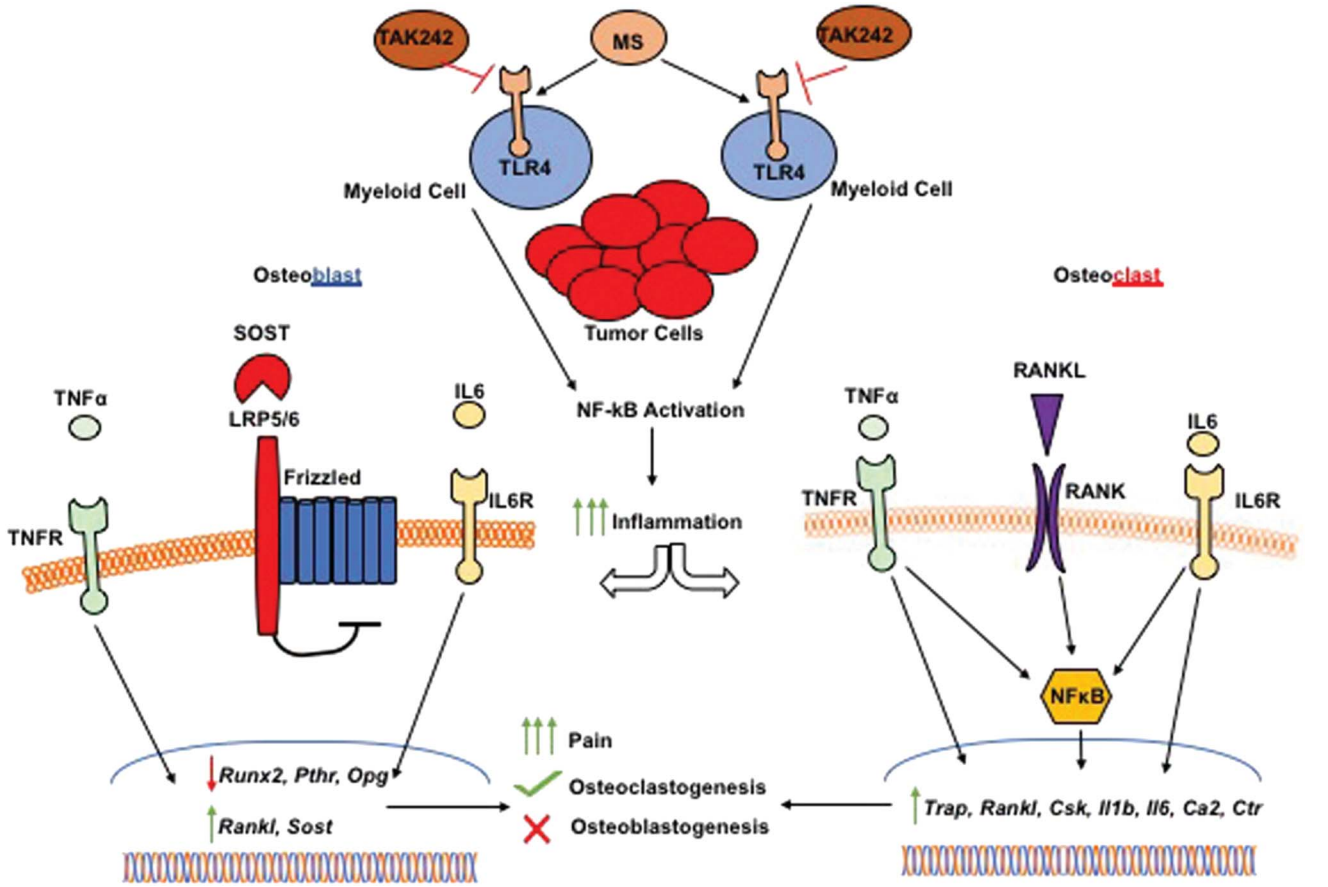

Figure 8. Schematic representation of proposed and theorized mechanism leading to morphine-induced hypersensitivity and enhanced osteolysis through TLR4 receptor activation. Chronic morphine administration is able to activate TLR4 primarily on immune cells within the bone-tumor microenvironment leading to downstream activation of NF-κB transcription factor. In the bone tumor microenvironment where there is an increased inflammatory response, this process can exacerbate production of inflammatory cytokines such as IL-6, TNFα, and IL-1β. These have differential effects on osteoclasts and osteoblasts. Chronic inflammation has a negative effect on osteoblastic differentiation and activity. Acting through multiple receptors including IL-6R and TNFR, the upregulation of genes such as sclerostin and RANKL lead to enhanced osteoclast activity, whereas the downregulation of *Runx2* leads to decreased osteoblast differentiation.[13,14,21,22,33] Alternatively, on osteoclasts there these same inflammatory factors lead to the upregulation of osteoclastic genes such as *Ca2*, *Trap*, *Sost*, and *Csk*, which results in enhanced bone resorption.[38,45,47,71] In addition, this upregulation in inflammatory genes leads to the promotion of inflammatory pain states and the enhanced bone loss leads to greater pain and risk of pathologic fracture. These effects are observed to be blocked by the TLR4 antagonist, TAK242. Ca2, carbonic anhydrase 2; Csk, cathepsin K; Ctr, calcitonin receptor; IL-1β, interleukin 1β; IL-6, interleukin 6; Opg, osteoprotegerin; Pthr, parathyroid hormone receptor; Rankl, receptor activator of NF-κB ligand; Runx2, runt-related transcription factor 2; Sost, sclerostin; TLR4, toll-like receptor-4; Trap, tartrate-resistant acid phosphatase.

cytokines that have previously described effects on both osteoblasts and osteoclasts that lead to increased bone destruction (**Fig. 8**).

For the first time, we provide evidence that chronic morphine produces a TLR4-dependent and opioid receptor-independent contributions to pain evolution and bone loss in cancer-induced bone pain using multiple breast cancer cell lines. We demonstrate that metastatic bone cancer may be a state that is predisposed to TLR4-dependent bone loss. In addition, we demonstrate that TLR4 also plays a mitigating role in the opioid-induced hypersensitivity phenomenon that is observed in the CIBP model, suggesting that exacerbated inflammation may be underlying this, in part. Opioid analgesics remain the gold standard for clinicians to control cancer-induced bone pain; our data do not suggest the need for removal of opioids from the treatment paradigm, but rather the need to develop alternative strategies that may mitigate some of the TLR4-dependent side effects. It is also necessary for more rigorous molecular and pharmacological investigations into the mechanisms of opioid-TLR4 interactions and signaling to more rationally design approaches to mitigate this issue. In addition, these observations have direct clinical impact as TAK242, clinically known as resatorvid, has already gone through FDA phase 3 trials for sepsis. Therefore, it could easily be repurposed and retested in clinical trials, in conjunction with opioid analgesics, to determine if it reduces opioid dosing, decreases hypersensitivity and tolerance, or decreases tumor degradation in patients with metastatic bone cancer. Overall, it is essential to create a more detailed understanding of opioid pharmacology not only at its known receptors, but the off-target sites to better treat patients and predict the therapeutic pitfalls that arise in the treatment of cancer-induced bone pain.

Conflict of interest statement

The authors have no conflicts of interest to declare.

Acknowledgements

This work was supported by the National Institutes of Health National Cancer Institute and National Institute on Drug Abuse [R01 CA14215, P30 DA051355] and by the Comprehensive Pain and Addiction Center (CPAC), University of Arizona Health

Sciences. E0771 cells were graciously provided by Kathryn Visser at the Olivia Newton-John Cancer Research Institute Metastasis Research Institute (Victoria, Australia).

All data are available in excel, Prizm, and radiographic images and can be accessed by a request to the corresponding author, T. W. Vanderah.

Author contributions: A. L. Thompson, S. A. Grenald, T. M. Largent-Milnes, and T. W. Vanderah were responsible for designing the research study. A. L. Thompson, S. A. Grenald, H. A. Ciccone, A. F. Smith, D. Mohty, D. S. Margolis, D. L. Coleman, E. De Leon, E. Bahramnejad, and L. Kasper-Conella were involved in conducting experiments and acquiring data. A. L. Thompson, S. A. Grenald, D. S. Margolis, T. M. Largent-Milnes, J. L. Uhrlab, and T. W. Vanderah were involved in data analysis. A. L. Thompson, D. Salvemini, D. S. Margolis, T. M. Largent-Milnes, and T. W. Vanderah all contributed to writing the manuscript.

Supplemental digital content

Supplemental digital content associated with this article can be found online at http://links.lww.com/PAIN/B854.

Article history:
Received 15 December 2022
Received in revised form 28 March 2023
Accepted 18 April 2023
Available online 15 June 2023

References

[1] AlQranei MS, Senbanjo LT, Aljohani H, Hamza T, Chellaiah MA. Lipopolysaccharide- TLR-4 axis regulates osteoclastogenesis independent of RANKL/RANK signaling. BMC Immunol 2021;22:23.
[2] Anract P, Biau D, Boudou-Rouquette P. Metastatic fractures of long limb bones. Orthop Traumatol Surg Res 2017;103:S41–51.
[3] Boland JW, Pockley AG. Influence of opioids on immune function in patients with cancer pain: from bench to bedside. Br J Pharmacol 2018; 175:2726–36.
[4] Boland JW, Ziegler L, Boland EG, McDermid K, Bennett MI. Is regular systemic opioid analgesia associated with shorter survival in adult patients with cancer? A systematic literature review. PAIN 2015;156:2152–63.
[5] Caraceni A, Martini C, Zecca E, Portenoy RK, Ashby MA, Hawson G, Jackson KA, Lickiss N, Muirden N, Pisasale M, Moulin D, Schulz VN, Rico Pazo MA, Serrano JA, Andersen H, Henriksen HT, Mejholm I, Sjogren P, Heiskanen T, Kalso E, Pere P, Poyhia R, Vuorinen E, Tigerstedt I, Ruismaki P, Bertolino M, Larue F, Ranchere JY, Hege-Scheuing G, Bowdler I, Helbing F, Kostner E, Radbruch L, Kastrinaki K, Shah S, Vijayaram S, Sharma KS, Devi PS, Jain PN, Ramamani PV, Beny A, Brunelli C, Maltoni M, Mercadante S, Plancarte R, Schug S, Engstrand P, Ovalle AF, Wang X, Alves MF, Abrunhosa MR, Sun WZ, Zhang L, Gazizov A, Vaisman M, Rudoy S, Gomez Sancho M, Vila P, Trelis J, Chaudakshetrin P, Koh ML, Van Dongen RT, Vielvoye-Kerkmeer A, Boswell MV, Elliott T, Hargus E, Lutz L; Working Group of an IASP Task Force on Cancer Pain. Breakthrough pain characteristics and syndromes in patients with cancer pain. An international survey. Palliat Med 2004;18:177–83.
[6] Carlson CL. Effectiveness of the World Health Organization cancer pain relief guidelines: an integrative review. J Pain Res 2016;9: 515–34.
[7] Centers for Disease Control and Prevention. Understanding the epidemic. Vol. 2021. CDC: Centers for Disesae Control and Prevention. Available at: https://www.cdc.gov/opioids/basics/epidemic.html#print Accessed June 1, 2022.
[8] Chang J, Wang Z, Tang E, Fan Z, McCauley L, Franceschi R, Guan K, Krebsbach PH, Wang CY. Inhibition of osteoblastic bone formation by nuclear factor-κB. Nat Med 2009;15:682–9.
[9] Chartier SR, Thompson ML, Longo G, Fealk MN, Majuta LA, Mantyh PW. Exuberant sprouting of sensory and sympathetic nerve fibers in nonhealed bone fractures and the generation and maintenance of chronic skeletal pain. PAIN 2014;155:2323–36.
[10] Chen X, Zhu G, Jin T, Zhou Z, Gu S, Qiu J, Xiao H. Cadmium stimulates the osteoclastic differentiation of RAW264.7 cells in presence of osteoblasts. Biol Trace Elem Res 2012;146:349–53.
[11] Chrastil J, Sampson C, Jones KB, Higgins TF. Evaluating the affect and reversibility of opioid-induced androgen deficiency in an orthopaedic animal fracture model. Clin Orthop Relat Res 2014;472:1964–71.
[12] Daniell HW. Opioid osteoporosis. Arch Intern Med 2004;164:338; author reply 338.
[13] Devlin RD, Reddy SV, Savino R, Ciliberto G, Roodman GD. IL-6 mediates the effects of IL-1 or TNF, but not PTHrP or 1,25(OH)2D3, on osteoclast-like cell formation in normal human bone marrow cultures. J Bone Miner Res 1998;13:393–9.
[14] Ding J, Ghali O, Lencel P, Broux O, Chauveau C, Devedjian JC, Hardouin P, Magne D. TNF-α and IL-1β inhibit RUNX2 and collagen expression but increase alkaline phosphatase activity and mineralization in human mesenchymal stem cells. Life Sci 2009;84:499–504.
[15] Domenis R, Cifu A, Marino D, Fabris M, Niazi KR, Soon-Shiong P, Curcio F. Toll-like receptor-4 activation boosts the immunosuppressive properties of tumor cells-derived exosomes. Sci Rep 2019;9:8457.
[16] Duarte RV, Raphael JH, Southall JL, Labib MH, Whallett AJ, Ashford RL. Hypogonadism and low bone mineral density in patients on long-term intrathecal opioid delivery therapy. BMJ Open 2013;3:e002856.
[17] Dursteler-MacFarland KM, Kowalewski R, Bloch N, Wiesbeck GA, Kraenzlin ME, Stohler R. Patients on injectable diacetylmorphine maintenance have low bone mass. Drug Alcohol Rev 2011;30: 577–82.
[18] Ellis A, Grace PM, Wieseler J, Favret J, Springer K, Skarda B, Ayala M, Hutchinson MR, Falci S, Rice KC, Maier SF, Watkins LR. Morphine amplifies mechanical allodynia via TLR4 in a rat model of spinal cord injury. Brain Behav Immun 2016;58:348–56.
[19] Engelmann C, Sheikh M, Sharma S, Kondo T, Loeffler-Wirth H, Zheng YB, Novelli S, Hall A, Kerbert AJC, Macnaughtan J, Mookerjee R, Habtesion A, Davies N, Ali T, Gupta S, Andreola F, Jalan R. Toll-like receptor 4 is a therapeutic target for prevention and treatment of liver failure. J Hepatol 2020;73:102–12.
[20] Forget P, Aguirre JA, Bencic I, Borgeat A, Cama A, Condron C, Eintrei C, Eroles P, Gupta A, Hales TG, Ionescu D, Johnson M, Kabata P, Kirac I, Ma D, Mokini Z, Guerrero Orriach JL, Retsky M, Sandrucci S, Siekmann W, Stefancic L, Votta-Vellis G, Connolly C, Buggy D. How anesthetic, analgesic and other non-surgical techniques during cancer surgery might affect postoperative oncologic outcomes: a summary of current state of evidence. Cancers (Basel) 2019;11:592.
[21] Gilbert L, He X, Farmer P, Rubin J, Drissi H, van Wijnen AJ, Lian JB, Stein GS, Nanes MS. Expression of the osteoblast differentiation factor RUNX2 (Cbfa1/AML3/Pebp2αA) is inhibited by tumor necrosis factor-α. J Biol Chem 2002;277:2695–701.
[22] Gilbert LC, Rubin J, Nanes MS. The p55 TNF receptor mediates TNF inhibition of osteoblast differentiation independently of apoptosis. Am J Physiol Endocrinol Metab 2005;288:E1011–8.
[23] Grey A, Rix-Trott K, Horne A, Gamble G, Bolland M, Reid IR. Decreased bone density in men on methadone maintenance therapy. Addiction 2011;106:349–54.
[24] Hanks GW, Conno F, Cherny N, Hanna M, Kalso E, McQuay HJ, Mercadante S, Meynadier J, Poulain P, Ripamonti C, Radbruch L, Casas JR, Sawe J, Twycross RG, Ventafridda V. Expert working group of the research network of the European association for palliative C. Morphine and alternative opioids in cancer pain: the EAPC recommendations. Br J Cancer 2001;84:587–93.
[25] Hill T, D'Alessandro P, Murray K, Yates P. Prognostic factors following pathological fractures. ANZ J Surg 2015;85:159–63.
[26] Hiraga T, Ninomiya T. Establishment and characterization of a C57BL/6 mouse model of bone metastasis of breast cancer. J Bone Miner Metab 2019;37:235–42.
[27] Hutchinson MR, Bland ST, Johnson KW, Rice KC, Maier SF, Watkins LR. Opioid-induced glial activation: mechanisms of activation and implications for opioid analgesia, dependence, and reward. Scientific World J 2007;7:98–111.
[28] Hutchinson MR, Zhang Y, Shridhar M, Evans JH, Buchanan MM, Zhao TX, Slivka PF, Coats BD, Rezvani N, Wieseler J, Hughes TS, Landgraf KE, Chan S, Fong S, Phipps S, Falke JJ, Leinwand LA, Maier SF, Yin H, Rice KC, Watkins LR. Evidence that opioids may have toll-like receptor 4 and MD-2 effects. Brain Behav Immun 2010;24:83–95.
[29] Ii M, Matsunaga N, Hazeki K, Nakamura K, Takashima K, Seya T, Hazeki O, Kitazaki T, Iizawa Y. A novel cyclohexene derivative, ethyl (6R)-6-[N-(2-Chloro-4-fluorophenyl)sulfamoyl]cyclohex-1-ene-1-carboxylate (TAK-242), selectively inhibits toll-like receptor 4-mediated cytokine production through suppression of intracellular signaling. Mol Pharmacol 2006;69:1288–95.

[30] Jacobsen JH, Watkins LR, Hutchinson MR. Discovery of a novel site of opioid action at the innate immune pattern-recognition receptor TLR4 and its role in addiction. Int Rev Neurobiol 2014;118:129–63.
[31] Johnson RW, Suva LJ. Hallmarks of bone metastasis. Calcif Tissue Int 2018;102:141–51.
[32] Juneja R. Opioids and cancer recurrence. Curr Opin Support Palliat Care 2014;8:91–101.
[33] Kaneki H, Guo R, Chen D, Yao Z, Schwarz EM, Zhang YE, Boyce BF, Xing L. Tumor necrosis factor promotes Runx2 degradation through up-regulation of Smurf1 and Smurf2 in osteoblasts. J Biol Chem 2006;281: 4326–33.
[34] Karin M, Greten FR. NF-κB: linking inflammation and immunity to cancer development and progression. Nat Rev Immunol 2005;5:749–59.
[35] Kawai T, Akira S. Signaling to NF-κB by toll-like receptors. Trends Mol Med 2007;13:460–9.
[36] Kawasaki T, Kawai T. Toll-like receptor signaling pathways. Front Immunol 2014;5:461.
[37] King T, Vardanyan A, Majuta L, Melemedjian O, Nagle R, Cress AE, Vanderah TW, Lai J, Porreca F. Morphine treatment accelerates sarcoma-induced bone pain, bone loss, and spontaneous fracture in a murine model of bone cancer. PAIN 2007;132:154–68.
[38] Kobayashi K, Takahashi N, Jimi E, Udagawa N, Takami M, Kotake S, Nakagawa N, Kinosaki M, Yamaguchi K, Shima N, Yasuda H, Morinaga T, Higashio K, Martin TJ, Suda T. Tumor necrosis factor alpha stimulates osteoclast differentiation by a mechanism independent of the ODF/RANKL-RANK interaction. J Exp Med 2000;191:275–86.
[39] Kolosov A, Aurini L, Williams ED, Cooke I, Goodchild CS. Intravenous injection of leconotide, an omega conotoxin: synergistic antihyperalgesic effects with morphine in a rat model of bone cancer pain. Pain Med 2011; 12:923–41.
[40] Krum SA, Chang J, Miranda-Carboni G, Wang CY. Novel functions for NFκB: inhibition of bone formation. Nat Rev Rheumatol 2010;6:607–11.
[41] Lee CH, Wu CL, Shiau AL. Toll-like receptor 4 signaling promotes tumor growth. J Immunother 2010;33:73–82.
[42] Lozano-Ondoua AN, Wright C, Vardanyan A, King T, Largent-Milnes TM, Nelson M, Jimenez-Andrade JM, Mantyh PW, Vanderah TW. A cannabinoid 2 receptor agonist attenuates bone cancer-induced pain and bone loss. Life Sci 2010;86:646–53.
[43] Lozano-Ondoua AN, Hanlon KE, Symons-Liguori AM, Largent-Milnes TM, Havelin JJ, Ferland HL III, Chandramouli A, Owusu-Ankomah M, Nikolich-Zugich T, Bloom AP, Jimenez-Andrade JM, King T, Porreca F, Nelson MA, Mantyh PW, Vanderah TW. Disease modification of breast cancer-induced bone remodeling by cannabinoid 2 receptor agonists. J Bone Miner Res 2013;28:92–107.
[44] Lozano-Ondoua AN, Symons-Liguori AM, Vanderah TW. Cancer-induced bone pain: mechanisms and models. Neurosci Lett 2013;557:52–9.
[45] Ma T, Miyanishi K, Suen A, Epstein NJ, Tomita T, Smith RL, Goodman SB. Human interleukin-1-induced murine osteoclastogenesis is dependent on RANKL, but independent of TNF-α. Cytokine 2004;26:138–44.
[46] Mantyh WG, Jimenez-Andrade JM, Stake JI, Bloom AP, Kaczmarska MJ, Taylor RN, Freeman KT, Ghilardi JR, Kuskowski MA, Mantyh PW. Blockade of nerve sprouting and neuroma formation markedly attenuates the development of late stage cancer pain. Neuroscience 2010;171: 588–98.
[47] Mason JJ, Williams BO. SOST and DKK: antagonists of LRP family signaling as targets for treating bone disease. J Osteoporos 2010;2010:1–9.
[48] Mercadante S. Problems of long-term spinal opioid treatment in advanced cancer patients. PAIN 1999;79:1–13.
[49] Ormsby NM, Leong WY, Wong W, Hughes HE, Swaminathan V. The current status of prophylactic femoral intramedullary nailing for metastatic cancer. Ecancermedicalscience 2016;10:698.
[50] Pippenger BE, Duhr R, Muraro MG, Pagenstert GI, Hugle T, Geurts J. Multicolor flow cytometry-based cellular phenotyping identifies osteoprogenitors and inflammatory cells in the osteoarthritic subchondral bone marrow compartment. Osteoarthritis Cartilage 2015; 23:1865–9.
[51] Raad M, Suresh KV, Puvanesarajah V, Forsberg J, Morris C, Levin A. The pathologic fracture mortality index: a novel externally validated tool for predicting 30-day postoperative mortality. J Am Acad Orthop Surg 2021; 29:e1264–73.
[52] Raisz LG, Mundy GR, Luben RA. Skeletal reactions to neoplasms. Ann N Y Acad Sci 1974;230:473–5.
[53] Redlich K, Smolen JS. Inflammatory bone loss: pathogenesis and therapeutic intervention. Nat Rev Drug Discov 2012;11:234–50.
[54] Remeniuk B, King T, Sukhtankar D, Nippert A, Li N, Li F, Cheng K, Rice KC, Porreca F. Disease modifying actions of interleukin-6 blockade in a rat model of bone cancer pain. PAIN 2018;159:684–98.
[55] Robertson KM, Norgard M, Windahl SH, Hultenby K, Ohlsson C, Andersson G, Gustafsson JA. Cholesterol-sensing receptors, liver × receptor α and β, have novel and distinct roles in osteoclast differentiation and activation. J Bone Miner Res 2006;21:1276–87.
[56] Salter DM, Robb JE, Wright MO. Electrophysiological responses of human bone cells to mechanical stimulation: evidence for specific integrin function in mechanotransduction. J Bone Miner Res 1997;12:1133–41.
[57] Schneider CA, Rasband WS, Eliceiri KW. NIH Image to ImageJ: 25 years of image analysis. Nat Methods 2012;9:671–5.
[58] Sharma A, Cohen HW, Freeman R, Santoro N, Schoenbaum EE. Prospective evaluation of bone mineral density among middle-aged HIV-infected and uninfected women: association between methadone use and bone loss. Maturitas 2011;70:295–301.
[59] Shorr RI, Griffin MR, Daugherty JR, Ray WA. Opioid analgesics and the risk of hip fracture in the elderly: codeine and propoxyphene. J Gerontol 1992;47:M111–5.
[60] Slosky LM, BassiriRad NM, Symons AM, Thompson M, Doyle T, Forte BL, Staatz WD, Bui L, Neumann WL, Mantyh PW, Salvemini D, Largent-Milnes TM, Vanderah TW. The cystine/glutamate antiporter system xc- drives breast tumor cell glutamate release and cancer-induced bone pain. PAIN 2016;157:2605–16.
[61] Teng Z, Zhu Y, Wu F, Zhu Y, Zhang X, Zhang C, Wang S, Zhang L. Opioids contribute to fracture risk: a meta-analysis of 8 cohort studies. PLoS One 2015;10:e0128232.
[62] Thompson AL, Largent-Milnes TM, Vanderah TW. Animal models for the study of bone-derived pain. Methods Mol Biol 2019;1914:391–407.
[63] Thompson AL, Grenald SA, Ciccone HA, BassiriRad N, Niphakis MJ, Cravatt BF, Largent-Milnes TM, Vanderah TW. The endocannabinoid system alleviates pain in a murine model of cancer-induced bone pain. J Pharmacol Exp Ther 2020;373:230–8.
[64] van den Beuken-van Everdingen MH, de Rijke JM, Kessels AG, Schouten HC, van Kleef M, Patijn J. Prevalence of pain in patients with cancer: a systematic review of the past 40 years. Ann Oncol 2007;18: 1437–49.
[65] Vanderah TW, Gardell LR, Burgess SE, Ibrahim M, Dogrul A, Zhong CM, Zhang ET, Malan TP Jr., Ossipov MH, Lai J, Porreca F. Dynorphin promotes abnormal pain and spinal opioid antinociceptive tolerance. J Neurosci 2000;20:7074–9.
[66] Vermeirsch H, Nuydens RM, Salmon PL, Meert TF. Bone cancer pain model in mice: evaluation of pain behavior, bone destruction and morphine sensitivity. Pharmacol Biochem Behav 2004;79:243–51.
[67] Vestergaard P, Rejnmark L, Mosekilde L. Fracture risk associated with the use of morphine and opiates. J Intern Med 2006;260:76–87.
[68] Walser TC, Rifat S, Ma X, Kundu N, Ward C, Goloubeva O, Johnson MG, Medina JC, Collins TL, Fulton AM. Antagonism of CXCR3 inhibits lung metastasis in a murine model of metastatic breast cancer. Cancer Res 2006;66:7701–7.
[69] Wang X, Loram LC, Ramos K, de Jesus AJ, Thomas J, Cheng K, Reddy A, Somogyi AA, Hutchinson MR, Watkins LR, Yin H. Morphine activates neuroinflammation in a manner parallel to endotoxin. Proc Natl Acad Sci U S A 2012;109:6325–30.
[70] Warfield CA. Controlled-release morphine tablets in patients with chronic cancer pain: a narrative review of controlled clinical trials. Cancer 1998; 82:2299–306.
[71] Winkler DG, Sutherland MK, Geoghegan JC, Yu C, Hayes T, Skonier JE, Shpektor D, Jonas M, Kovacevich BR, Staehling-Hampton K, Appleby M, Brunkow ME, Latham JA. Osteocyte control of bone formation via sclerostin, a novel BMP antagonist. EMBO J 2003;22:6267–76.
[72] Wu C, Ding X, Zhou C, Ye P, Sun Y, Wu J, Zhang A, Huang X, Ren L, Wang K, Deng P, Yue Z, Chen J, Wang S, Xia J. Inhibition of intimal hyperplasia in murine aortic allografts by administration of a small-molecule TLR4 inhibitor TAK-242. Sci Rep 2017;7:15799.
[73] Xiao Y, Song JY, de Vries TJ, Fatmawati C, Parreira DB, Langenbach GE, Babala N, Nolte MA, Everts V, Borst J. Osteoclast precursors in murine bone marrow express CD27 and are impeded in osteoclast development by CD70 on activated immune cells. Proc Natl Acad Sci U S A 2013;110:12385–90.
[74] Zhang H, Lund DM, Ciccone HA, Staatz WD, Ibrahim MM, Largent-Milnes TM, Seltzman HH, Spigelman I, Vanderah TW. Peripherally restricted cannabinoid 1 receptor agonist as a novel analgesic in cancer-induced bone pain. PAIN 2018;159:1814–23.
[75] Zhang R, Dong Y, Sun M, Wang Y, Cai C, Zeng Y, Wu Y, Zhao Q. Tumor-associated inflammatory microenvironment in non-small cell lung cancer: correlation with FGFR1 and TLR4 expression via PI3K/Akt pathway. J Cancer 2019;10:1004–12.
[76] Zhong X, Xiao Q, Liu Z, Wang W, Lai CH, Yang W, Yue P, Ye Q, Xiao J. TAK242 suppresses the TLR4 signaling pathway and ameliorates DCD liver IRI in rats. Mol Med Rep 2019;20:2101–10.